



UNIVERSITÀ  
DEGLI STUDI  
DI PADOVA

*Università degli Studi di Padova*

*Padua Research Archive - Institutional Repository*

Diabetic Macular Edema With and Without Subfoveal Neuroretinal Detachment: Two Different Morphologic and Functional Entities

*Original Citation:*

*Availability:*

This version is available at: 11577/3240217 since: 2018-03-15T18:23:44Z

*Publisher:*

*Published version:*

DOI: 10.1016/j.ajo.2017.06.026

*Terms of use:*

Open Access

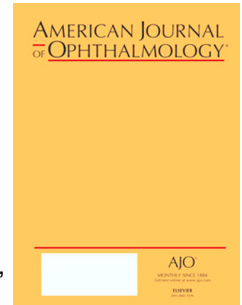
This article is made available under terms and conditions applicable to Open Access Guidelines, as described at <http://www.unipd.it/download/file/fid/55401> (Italian only)

(Article begins on next page)

# Accepted Manuscript

Diabetic macular edema with and without subfoveal neuroretinal detachment: two different morphological and functional entities

Stela Vujosevic, MD, PhD, Tommaso Torresin, MD, Marianna Berton, MD, Silvia Bini, MD, Enrica Convento, MSc, Edoardo Midena, MD, PhD



PII: S0002-9394(17)30280-5

DOI: [10.1016/j.ajo.2017.06.026](https://doi.org/10.1016/j.ajo.2017.06.026)

Reference: AJOPHT 10184

To appear in: *American Journal of Ophthalmology*

Received Date: 15 February 2017

Revised Date: 17 June 2017

Accepted Date: 26 June 2017

Please cite this article as: Vujosevic S, Torresin T, Berton M, Bini S, Convento E, Midena E, Diabetic macular edema with and without subfoveal neuroretinal detachment: two different morphological and functional entities, *American Journal of Ophthalmology* (2017), doi: 10.1016/j.ajo.2017.06.026.

This is a PDF file of an unedited manuscript that has been accepted for publication. As a service to our customers we are providing this early version of the manuscript. The manuscript will undergo copyediting, typesetting, and review of the resulting proof before it is published in its final form. Please note that during the production process errors may be discovered which could affect the content, and all legal disclaimers that apply to the journal pertain.

**Diabetic macular edema with and without subfoveal neuroretinal detachment: two different morphological and functional entities**

**Stela Vujosevic MD, PhD <sup>1</sup>, Tommaso Torresin MD <sup>1</sup>, Marianna Berton MD <sup>1</sup>, Silvia Bini MD <sup>1</sup>, Enrica Convento MSc <sup>1</sup>, Edoardo Midena MD, PhD <sup>1,2</sup>**

1 Department of Ophthalmology, University of Padova, Italy

2 Fondazione G. B. Bietti, IRCCS, Roma, Italy

Corresponding Author: Prof. Edoardo Midena MD, PhD

Department of Ophthalmology University of Padova

Via Giustiniani 2, 35128 Padova

Tel: +39498212394

Fax: +39498755168

Email: edoardo.midena@unipd.it

**Short title:** Diabetic macular edema with neuroretinal detachment

**Abstract:**

**Purpose:** To assess specific morphologic and functional characteristics in eyes with diabetic macular edema (DME) with subfoveal neuroretinal detachment (SND+) vs DME without SND (SND-).

**Design:** Cross-sectional, prospective, comparative case series.

**Methods:** Seventy two patients (72 eyes: 22 eyes SND+ and 50 eyes SND-) with treatment-naïve, center-involving DME were evaluated. Data gathering included fundus color photographs, fluorescein angiography, spectral-domain optical coherence tomography (SD-OCT), best corrected visual acuity (BCVA), and microperimetry. The following parameters were evaluated with SD-OCT: central macular thickness (CMT, including SND); central retinal thickness (CRT, excluding SND); choroidal thickness (CT); nasal and temporal retinal thickness (RT) at 500  $\mu$ m and 1500  $\mu$ m from the fovea; the number of hyper-reflective retinal spots (HRS) in the central 3000  $\mu$ m; and the presence of SND and integrity of the external limiting membrane (ELM). Retinal sensitivity (RS) was evaluated within 4° and 12° of the fovea. Correlation among CT, RS, and HRS in patients with and without SND was determined.

**Results:** CMT ( $P=0.032$ ), temporal RT at 1500  $\mu$ m ( $P=0.03$ ), mean CT ( $P=0.009$ ) and mean number of HRS ( $P=0.0001$ ) were all higher in SND+ vs SND- eyes. CRT, BCVA, HbA1c, and prevalence of systemic arterial hypertension were not different between the two groups. RS within 4° ( $P=0.002$ ) and 12° ( $P=0.015$ ) was lower in SND+ vs SND- eyes. SND correlated significantly with disruption of the ELM (54.55% vs 24%,  $P=0.01$ ) and lower RS. A direct correlation was found between the number of HRS, presence of SND, CT, and RS within 12° in SND- eyes, and an inverse correlation was found between CT and RS within 12° in SND+ eyes.

**Conclusions:** This data may improve characterization of DME in eyes with SND. DME with SND correlates with greater CT, more HRS, disruption of the ELM and significant macular functional impairment (RS decrease) vs SND-.

**INTRODUCTION**

Diabetic macular edema (DME) presents with different patterns on optical coherence tomography (OCT) including sponge-like swelling, cystoid macular edema, and subfoveal neuroretinal detachment (SND).<sup>1</sup> SND in DME is visible on OCT as a hypo-reflective area beneath the neuroretina and with a reported prevalence of approximately 15-30% in eyes with DME.<sup>1-5</sup> Recently, higher concentrations of inflammatory cytokines in the vitreous and aqueous humor have been reported in eyes with SND, thus suggesting the presence of a significant inflammatory component.<sup>5-9</sup> In particular, an increase in interleukin 6 (IL-6) has been associated with SND in DME.<sup>5</sup> Some authors have reported a poorer visual prognosis after treatment of eyes with SND.<sup>10,11</sup>

Different hypotheses regarding the pathophysiology of SND have been postulated for this specific pattern of DME.<sup>1-4,12,13</sup> Leakage from the retinal or choroidal circulation into the subretinal space that exceeds reabsorption capacity is thought to be the main mechanism.<sup>14</sup> Several authors have reported retinal pigment epithelium (RPE) dysfunction in experimental and human diabetes,<sup>15-17</sup> as RPE pumping capacity is decreased by hypoxia.<sup>18</sup> Moreover, an impairment of choroidal blood flow, which may

cause tissue hypoxia and RPE dysfunction, was reported in patients with DME.<sup>12</sup> Also the integrity of the external limiting membrane (ELM) appears to contribute to the pathogenesis of SND. In fact, integrity of the ELM seems to be a key factor in preventing fluid passing from the outer retina into subretinal space.<sup>2</sup>

The formation of SND is not associated with the duration or severity of DME.<sup>2</sup> Otani et al. postulated that transient SND may represent fluid movement from the retina to the subretinal space during the process of macular edema absorption.<sup>10</sup> Gaucher et al. reported that SND can occur very early in the genesis of DME, even before the accumulation of a large amount of fluid in the macula.<sup>2</sup> SND may disappear both before or after the reabsorption of intraretinal fluid, thereby suggesting that SND is not associated with severe DME.<sup>2</sup> Therefore, SND does not seem to be due to only the passive reabsorption of DME.<sup>2</sup>

Since little is known about the pathophysiology and the clinical characteristics of DME with SND, the main purpose of this study was to evaluate in detail morphologic and functional characteristics of patients with SND (SND+) and compare these to DME without SND (SND-).

## **MATERIALS AND METHODS**

### **Population**

This is a cross-sectional, prospective, comparative, consecutive case series of 72 eyes (72 patients) with treatment-naïve, center-involving DME. All patients underwent a complete ophthalmologic examination with best corrected visual acuity determination (BCVA), color fundus photographs, spectral domain optical coherence tomography (SD-OCT), fluorescein angiography, and microperimetry. Exclusion criteria were any previous macular/retinal treatment (laser, intravitreal injections, and surgery), presence of macular traction on SD-OCT, history of uncontrolled glaucoma or ocular hypertension, and ischemic maculopathy. Informed consent was obtained from each patient and the research was carried out in accordance with the Declaration of Helsinki. Local Ethics Committee approval for the study was obtained.

### **Visual acuity**

Best corrected visual acuity was measured by a certified examiner using the standard Early Treatment Diabetic Retinopathy Study (ETDRS) protocol at a distance of 4 meters with a modified trans-illuminated ETDRS distance chart (Precision Vision, Bloomington, IL). Visual acuity was scored as the total number of letters read correctly, calculated according to the ETDRS score method, and annotated in the clinical chart.

### **Spectral Domain Optical Coherence Tomography**

Spectral domain OCT was performed with the Spectralis (Heidelberg Engineering, Heidelberg, Germany; Software 5.3.0.15), with the following scan patterns: one linear scan of 8.8 mm at 0° centered on the fovea in High Speed mode and in Enhanced Depth Imaging (EDI) mode with a resolution of 100 automatic real time (ART), and a 6x6 mm macular map with resolution of 50 ART, centered on the fovea. Measurements made with the Heidelberg Eye Explorer software (EYEX™) included the presence and

height of SND, central macular thickness (CMT) (automatically measured within 1 central mm including also the SND), and central retinal thickness (obtained excluding the SND, by measuring the SND height), nasal and temporal thickness of the inner retina (IRT) and the outer retina (ORT) at 500  $\mu$ m and 1500  $\mu$ m from the fovea (IRT was measured from the inner limiting membrane to the outer plexiform layer).

The following parameters were also measured: ORT from the outer nuclear layer to the retinal pigment epithelium; the total number of retinal hyper-reflective spots (HRS) (calculated in the area of 3000  $\mu$ m centered on the fovea); integrity of the external limiting membrane (ELM) within the 3 central mm; choroidal thickness measured at the fovea (foveal CT), and at 500  $\mu$ m and 1500  $\mu$ m from the fovea on the nasal and temporal side; and mean CT (mean value of 5 measured values: foveal CT, nasal and temporal CT at 500  $\mu$ m and 1500  $\mu$ m) on linear B-Scans obtained with EDI mode passing through the center of the fovea at 0 degrees (Figures 1 and 2).

### **Microperimetry**

Microperimetry was performed on all subjects using the MP1 Microperimeter (Nidek, Gamagori, Japan). The following standard parameters were used for DME patients: a fixation target consisting of a red ring, 1° in diameter; white, monochromatic background at 4 asb; stimulus size of Goldman III, with 200 msec projection time; customized radial grid of 45 stimuli covering the central 12° (centered onto the fovea), 1° apart (inner stimuli) and 2° apart (outer stimuli).<sup>19</sup>

The starting stimulus light attenuation was set at 10 dB. A 4-2 double staircase strategy was used with an automatic eye tracker that compensates for eye movements. Pre-test training was performed and five minute mesopic visual adaptation was allowed before starting the test. All subjects underwent microperimetry with dilated pupils. Mean retinal sensitivity was evaluated within the central 4° and 12°, approximately covering 1 mm and 3 mm of the central retina area on OCT mapping.<sup>19</sup> Fixation stability and location were evaluated by the Fujii et al classification (stable, relatively unstable, and unstable; central, relatively eccentric, and eccentric fixation).<sup>20</sup>

### **Fluorescein angiography**

Fluorescein angiography was performed with the Heidelberg Retinal Angiograph 2 (HRA 2, Heidelberg Engineering, Heidelberg, Germany). Angiography images were evaluated for the presence of significant retinal capillary dropout in the macula. All measurements were evaluated independently by two masked graders. In case of disagreement, a final adjudication was made by the senior retina specialist.

### **Statistics**

Fisher's exact test was used to compare the prevalences of hypertension in SND+ and SND- patients. Mean HbA1c values were compared by student t-test for independent samples. Mean values of CMT, CRT, RT, CT, RS and number of HRS were compared between groups by student t-test for independent samples. The location and stability of fixation were evaluated by Fisher's exact test. Correlation between the number of HRS

and presence of SND was evaluated by a multiple logistic regression model with stepwise selection of determinants.

Spearman correlation coefficient was used to assess the correlation between CT and RS within 12 degrees, CT and number of HRS, RS within 12 degrees, and the number of HRS separately in SND- and SND+ eyes. A correlation coefficient of  $>0.20$  was considered clinically relevant.

To test the effect of SND on the relationship between CT and RS, a linear regression model with CT as the dependent variable and RS as a covariate interacting with the SND subgroup was applied. A significant interaction term indicated that correlation between the two subgroups of patients was unequal. The same model was applied to the relationship between the HRS and RS, as well as HRS and CT. Because the distribution of these variables was skewed, the ranks of measurements, instead of original values, were used. Association between SND height and stability of fixation was evaluated by the Wilcoxon-Mann-Whitney test (normal approximation with continuity correction of 0.5). Correlations between ELM integrity and the presence and height of SND were evaluated by the Chi-square and Wilcoxon-Mann-Whitney tests (normal approximation with continuity correction of 0.5) respectively.

For all statistical analyses, SAS<sup>®</sup> 9.3 on personal computer statistical software was used. P values less than 0.05 were interpreted as statistically significant.

## RESULTS

### Demographics

A total of 72 eyes of 72 patients were evaluated, 22 eyes were SND+ and 50 eyes were SND-. There was no significant difference in mean HbA1c levels and systemic arterial hypertension between SND+ and SND- patients (7.4% vs. 7.5%,  $P=0.71$ ;  $P=0.27$ , Fisher's exact test).

### Comparisons between OCT measurements and SND

Mean values of CMT (including SND), central retinal thickness (CRT, excluding SND) inner and outer RT at 500  $\mu\text{m}$  and 1500  $\mu\text{m}$  from the fovea both at the nasal and the temporal side, CT, and number of HRS are listed in Table 1. CMT, foveal CT and mean CT were significantly higher in SND+ eyes versus SND- eyes ( $P=0.0320$ ,  $P=0.0285$  and  $P=0.0098$ , respectively). CRT was not different between SND+ eyes and SND- eyes ( $P=0.2315$ ). The number of HRS was significantly higher in SND+ than SND- eyes ( $P<0.0001$ ).

In Table 2 are shown the mean values of the following functional parameters: BCVA, retinal sensitivity (RS) within the central 4° and 12°, and fixation characteristics (fixation stability and location). RS was lower in SND+ eyes both within the central 4° ( $p=0.0024$ ) and 12° ( $p=0.0152$ ). There was a significant difference in fixation stability between SND+ and SND- eyes ( $P=0.0035$ ). Fixation was predominantly central in both groups.



A direct and statistically significant correlation was found between the number of HRS and the presence of SND (odds ratio=1.05; 95% confidence limits 1.01-1.09;  $P=0.017$ ).

Results in Table 3 show a statistically significant correlation between mean CT in the macula and RS within 12° in SND- eyes (Spearman correlation,  $\rho=0.455$ ,  $P=0.022$ ), whereas an inverse, although not statistically significant, correlation was seen in SND+ eyes (Spearman correlation,  $\rho=-0.365$ ,  $P=0.300$ ). HRS were inversely correlated to RS in SND- eyes (Spearman correlation,  $\rho=-0.415$ ,  $P=0.039$ ) but no significant correlation was found between HRS and RS in SND+ eyes.

Mean SND height was 115  $\mu\text{m}$  (median: 99  $\mu\text{m}$ ; range: 20-280  $\mu\text{m}$ ). Table 4 shows the correlation between SND height and morphological parameters (mean CT, CMT, and CRT) and functional parameters (BCVA, RS within 4° and 12°). SND height was inversely correlated only to RS. In addition, SND height was not correlated to the stability of fixation (Wilcoxon-Mann-Whitney test,  $P=1.000$ ).

### External Limiting Membrane

The external limiting membrane (ELM) was intact in 48 eyes and disrupted in 24 eyes. In the group of SND+ eyes, the ELM was intact in 10 (45.45%) and disrupted in 12 (54.55%), whereas in the group of SND- eyes, ELM was intact in 38 (76%) and disrupted in 12 (24%). The presence of SND was significantly correlated with disruption of the ELM (54.55% vs 24%; Chi square test,  $P=0.0113$ ). Moreover, the mean height of the SND was greater in eyes with disrupted ELM versus eyes with intact ELM (141.3  $\mu\text{m}$  vs. 84.4  $\mu\text{m}$ ,  $P=0.051$ ).

## DISCUSSION

In this study we evaluated and compared specific morphologic and functional characteristics of patients with treatment-naïve, center-involving DME, with and without SND. More specifically, CMT, CRT, inner and outer retinal thickness, HRS and CT as morphologic parameters, and BCVA, retinal sensitivity, and fixation characteristics (determined by microperimetry) as functional parameters, were evaluated.

The main reason to evaluate these specific features was to obtain more information on, and better understand, the clinical characteristics of eyes with SND due to DME. In the present study SND was seen in 22 of 72 eyes (30.5%), which is in line with previous reports.<sup>2-4</sup> The major difference in retinal thickness between SND+ and SND- eyes was found in the CMT, whereas there was no significant difference in CRT and inner or outer retinal thickness (IRT, ORT) in the perifoveal region. Since there was no difference in the CRT between SND+ and SND- eyes, the difference in CMT measurements is due to the presence of subretinal fluid (extracellular fluid pooling between the outer segments of the photoreceptors and RPE). In this cohort of patients there was no significant difference in intraretinal thickness.

The choroid was significantly thicker in SND+ eyes vs SND- eyes, both in the fovea as well as in the nasal perifoveal area. Data in the literature regarding CT in eyes with



DME are conflicting. Whereas most authors report a decrease or no change in CT in eyes with DME,<sup>12,21-26</sup> others report an increase in CT in DME eyes.<sup>27,28</sup> Kim et al. reported increased subfoveal choroidal thickness in eyes with DME and SND compared to DME without SND.<sup>28</sup> This was confirmed in the present study. Thus, the present data may indicate that differences in DME and CT patterns may be attributed to different populations. Data from the present study (increased CT in treatment-naïve DME eyes associated with SND) confirm the hypothesis by Campos et al that SND is more likely to occur in early onset DME associated with increased CT, increased choriocapillaris permeability and outer blood-retinal barrier (BRB) dysfunction.<sup>29</sup> Therefore, the association of CT with different DME patterns merits further study.

In this study glycemic control and arterial hypertension did not correlate with the presence of SND, thus suggesting that local (intraocular) factors might be more important to the development of SND.

The pathophysiology by which SND forms is not yet fully understood, but one of the proposed mechanisms includes the condition of the ELM.<sup>4</sup> Breakdown of the inner BRB in eyes with DME causes an extravasation of lipids and proteins, but proteins and cells have difficulty passing through an intact ELM. Thus, they accumulate anterior to the ELM, resulting in swelling of the outer retina. When the ELM is compromised, proteins and fluid in the outer retina may move more easily into the subretinal space. These changes result in the development of SND.<sup>1</sup> Data from the present study confirms this, where disrupted ELM is correlated with the presence and height of SND in eyes with DME.

Disruption of the ELM in eyes with DME can be accompanied by cell damage, which attracts scavenger cells to the retina. These cells may be a source of IL-6.<sup>1,6</sup> In fact, SND has been correlated with higher intravitreal levels of IL-6, thus indicating a heightened “inflammatory condition”.<sup>1</sup> Increased concentrations of inflammatory cytokines and chemokines have been reported in the vitreous and aqueous humor of patients with DME.<sup>5,8,30,31</sup> Increased synthesis of cytokines by activated retinal glial cells result in elevated aqueous humor concentrations, even during the early stages of DR.<sup>30</sup>

Hyper-reflective retinal spots (HRS) on SD-OCT have been proposed as clinical signs of activated microglial cell aggregates in the retina.<sup>19,32-35</sup> The HRS, proposed as an imaging biomarker of retinal inflammation in eyes with DME, have the following characteristics: small size (<30 microns); reflectivity similar to the nerve fiber layer; located in both the inner but mostly in the outer retina; and no back-shadowing. These characteristics have been studied and validated previously.<sup>35</sup> The present study confirms previously published data that showed a significant increase in the number of HRS in SND+ eyes vs. SND- eyes.<sup>19</sup> Moreover, in the present study a direct and significant correlation was found between the HRS number and the presence of SND, thus strengthening the hypothesis of a “major inflammatory condition” in this pattern of DME.

Functional parameters (retinal sensitivity and fixation stability), showed greater visual impairment in SND+ eyes versus SND- eyes. Moreover, a greater SND height correlated with decreased RS. Deak et al. reported that SND and large cysts in the

outer nuclear layer are the two morphologic changes with the greatest negative impact on retinal sensitivity in DME.<sup>36</sup> Seo et al reported no differences in BCVA based on different OCT patterns (cystoid, diffuse, and with SND) at baseline, but only the SND type had a poorer functional response after anti-VEGF treatment.<sup>37</sup> In the present study there was no difference in BCVA between SND+ eyes and SND- eyes.

An inverse correlation was found between choroidal thickness and retinal sensitivity in SND+ eyes, whereas a direct correlation was found between CT and RS in SND- eyes. This is a peculiar finding that probably indicates that DME with SND+ and SND- are two different morphologic and functional entities. Although no final conclusions can be drawn (due to the limited number of examined eyes and no longitudinal data), it suggests that different patterns of DME that can be easily visualized with non-invasive imaging instruments such as SD-OCT should be more closely evaluated. The role of the choroid in DME may be related to the nature of the “retinal inflammatory condition” and may determine the morphologic pattern of DME, such as the presence of SND. Also the integrity of the ELM should be evaluated in SND+ eyes, since its disruption may indicate a poorer functional outcome. Moreover, functional impairment (retinal sensitivity) in eyes with SND+ and SND- may indicate the importance of the choroid on retinal sensitivity and fixation deterioration, and not just the presence of retinal edema. A longitudinal study evaluating these specific characteristics in relation to local treatment might provide more information on therapeutic outcomes in different patterns of DME, particularly those with SND.

#### ACKNOWLEDGMENTS/DISCLOSURE

A) Funding/Support: None

B) Financial Disclosures: No financial disclosures for any of the Authors.

C) Other Acknowledgements: The Authors would like to thank Fabiano Cavarzeran for his help in the statistical analyses of the data.

#### References

1. Otani T, Kishi S, Maruyama Y. Patterns of diabetic macular edema with optical coherence tomography. *Am J Ophthalmol*. 1999;127(6):688-93.
2. Gaucher D, Sebah C, Erginay A, Haouchine B, Tadayoni R, Gaudric A, Massin P. Optical coherence tomography features during the evolution of serous retinal detachment in patients with diabetic macular edema. *Am J Ophthalmol*. 2008;145(2):289-296.
3. Catier A, Tadayoni R, Paques M, et al. Characterization of macular edema from various etiologies by optical coherence tomography. *Am J Ophthalmol*. 2005;140(2):200–206.
4. Ozdemir H, Karacorlu M, Karacorlu S. Serous macular detachment in diabetic cystoid macular oedema. *Acta Ophthalmol Scand*. 2005;83(1):63–66.
5. Sonoda S, Sakamoto T, Yamashita T, Shirasawa M, Otsuka H, Sonoda Y. Retinal morphologic changes and concentrations of cytokines in eyes with diabetic macular edema. *Retina*. 2014;34(4):741-8.
6. Funatsu H, Yamashita H, Noma H, Mimura T, Yamashita T, Hori S. Increased levels of vascular endothelial growth factor and interleukin-6 in the aqueous humor of diabetics with macular edema. *Am J Ophthalmol*. 2002;133(1):70-7.
7. Funatsu H, Yamashita H, Sakata K, Noma H, Mimura T, Suzuki M, Eguchi S, Hori S. Vitreous levels of vascular endothelial growth factor and intercellular adhesion molecule 1 are related to diabetic macular edema. *Ophthalmology*. 2005;112(5):806-16.
8. Funatsu H, Noma H, Mimura T, Eguchi S, Hori S. Association of vitreous inflammatory factors with diabetic macular edema. *Ophthalmology*. 2009;116(1):73-9.
9. Sohn HJ, Han DH, Kim IT, Oh IK, Kim KH, Lee DY, Nam DH. Changes in aqueous concentrations of various cytokines after intravitreal triamcinolone versus bevacizumab for diabetic macular edema. *Am J Ophthalmol*. 2011;152(4):686-94.
10. Otani T, Kishi S. Tomographic assessment of vitreous surgery for diabetic macular edema. *Am J Ophthalmol*. 2000;129(4):487–494.
11. Seo KH, Yu SY, Kim M, Kwak HW. Visual and morphologic outcomes of intravitreal ranibizumab for diabetic macular edema based on optical coherence tomography patterns. *Retina*. 2016;36(3):588-95.
12. Nagaoka T, Kitaya N, Sugawara R, et al. Alteration of choroidal circulation in the foveal region in patients with type 2 diabetes. *Br J Ophthalmol*. 2004;88(8):1060–1063.
13. Marmor MF. Control of subretinal fluid and mechanisms of serous detachment. In: Marmor MF, Wolfensberger TJ, editors. *The retinal pigment epithelium: function and disease*. New York, NY: Oxford University Press; 1998:420–437.
14. Weinberg D, Jampol LM, Schatz H & Brady KD. Exudative retinal detachment following central and hemicentral retinal vein occlusions. *Arch Ophthalmol*. 1990;108(2):271–275.
15. Kirber WM, Nichols CW, Grimes PA, Winegrad AI, Laties AM. A permeability defect of the retinal pigment epithelium. Occurrence in early streptozocin diabetes. *Arch Ophthalmol*. 1980;98(4):725–728.

16. Grimes PA, Laties AM. Early morphological alteration of the pigment epithelium in streptozotocin-induced diabetes: increased surface area of the basal cell membrane. *Exp Eye Res.* 1980;30(6):631–639.
17. Weinberger D, Fink-Cohen S, Gatton DD, Priel E, Yassur Y. Non-retinovascular leakage in diabetic maculopathy. *Br J Ophthalmol.* 1995;79(8):728–731.
18. Spaide R, Yannuzzi L. Manifestations and pathophysiology of serous detachment of the retinal pigment epithelium and retina. In: Marmor M, Wolfensberger T, editors. *The retinal pigment epithelium: function and disease.* New York, NY: Oxford University Press; 1998:439–455.
19. Vujosevic S, Torresin T, Bini S, Convento E, Pilotto E, Parrozzani R, Midena E. Imaging retinal inflammatory biomarkers after intravitreal steroid and anti-VEGF treatment in diabetic macular oedema [published online ahead of print October 24 2016]. *Acta Ophthalmol.* doi:10.1111/aos.13294.
20. Fujii GY, De Juan E Jr, Sunness J, et al. Patient selection for macular translocation surgery using the scanning laser ophthalmoscope. *Ophthalmology.* 2002;109(9):1737–1744.
21. Querques G, Lattanzio R, Querques L, Del Turco C, Forte R, Pierro L, Souied EH, Bandello F. Enhanced depth imaging optical coherence tomography in type 2 diabetes. *Invest Ophthalmol Vis Sci.* 2012;53(10):6017–24.
22. Regatieri CV, Branchini L, Carmody J, Fujimoto JG, Duker JS. Choroidal thickness in patients with diabetic retinopathy analyzed by spectral-domain optical coherence tomography. *Retina.* 2012;32(3):563–8.
23. Adhi M, Brewer E, Waheed NK, Duker JS. Analysis of morphological features and vascular layers of choroid in diabetic retinopathy using spectral-domain optical coherence tomography. *JAMA Ophthalmol.* 2013;131(10):1267–74.
24. Vujosevic S, Martini F, Cavarzeran F, Pilotto E, Midena E. Macular and peripapillary choroidal thickness in diabetic patients. *Retina.* 2012;32(9):1781–90.
25. Lee HK, Lim JW, Shin MC. Comparison of choroidal thickness in patients with diabetes by spectral-domain optical coherence tomography. *Korean J Ophthalmol.* 2013;27(6):433–9.
26. Esmaeelpour M, Považay B, Hermann B, Hofer B, Kajic V, Hale SL, North RV, Drexler W, Sheen NJ. Mapping choroidal and retinal thickness variation in type 2 diabetes using three-dimensional 1060-nm optical coherence tomography. *Invest Ophthalmol Vis Sci.* 2011;52(8):5311–6.
27. Hua R, Liu L, Wang X, Chen L. Imaging evidence of diabetic choroidopathy in vivo: angiographic pathoanatomy and choroidal-enhanced depth imaging. *PLoS One.* 2013;8(12):e83494.
28. Kim JT, Lee DH, Joe SG, Kim JG, Yoon YH. Changes in choroidal thickness in relation to the severity of retinopathy and macular edema in type 2 diabetic patients. *Invest Ophthalmol Vis Sci.* 2013;54(5):3378–84.
29. Campos A, Campos EJ, Martins J, Ambrósio AF, Silva R. Viewing the choroid: where we stand, challenges and contradictions in diabetic retinopathy and diabetic macular oedema [Epub ahead of print]. *Acta Ophthalmol.* 2016. doi: 10.1111/aos.13210.
30. Vujosevic S, Micera A, Bini S, Berton M, Esposito G, Midena E. Proteome analysis of retinal glia cells-related inflammatory cytokines in the aqueous humour of diabetic patients. *Acta Ophthalmol.* 2016;94(1):56–64.

31. Dong N, Xu B, Chu L, Tang X. Study of 27 Aqueous Humor Cytokines in Type 2 Diabetic Patients with or without Macular Edema. *PLoS One*. 2015;10(4):e0125329.
32. Coscas G, De Benedetto U, Coscas F, Li Calzi CI, Vismara S, Roudot-Thoraval F, Bandello F, Souied E. Hyperreflective dots: a new spectral-domain optical coherence tomography entity for follow-up and prognosis in exudative age-related macular degeneration. *Ophthalmologica*. 2013;229(1):32-7.
33. Vujosevic S, Bini S, Midena G, Berton M, Pilotto E, Midena E. Hyperreflective intraretinal spots in diabetics without and with nonproliferative diabetic retinopathy: an in vivo study using spectral domain OCT. *J Diabetes Res*. 2013;2013:491835.
34. Vujosevic S, Berton M, Bini S, Casciano M, Cavarzeran F, Midena E. Hyperreflective retinal spots and visual function after anti-vascular endothelial growth factor treatment in center-involving diabetic macular edema. *Retina*. 2016;36(7):1298-308.
35. Vujosevic S, Bini S, Torresin T, et al. Hyperreflective retinal spots in normal and diabetic eyes: B-Scan and En Face Spectral Domain Optical Coherence Tomography Evaluation [published online ahead of print September 23 2016]. *Retina*. doi:10.1097/iae.0000000000001304
36. Deák GG, Bolz M, Ritter M, Prager S, Benesch T, Schmidt-Erfurth U; Diabetic Retinopathy Research Group Vienna. A systematic correlation between morphology and functional alterations in diabetic macular edema. *Invest Ophthalmol Vis Sci*. 2010;51(12):6710-4.
37. Seo Kh, Yu Sy, Kim M, Kwak H. Visual and morphologic outcomes of intravitreal ranibizumab for diabetic macular edema based on optical coherence tomography patterns. *Retina*. 2016;36(3):588-95.

### Legends of the Figures

**Figure 1.** Right eye of a patient with diabetic macular edema and subfoveal neuroretinal detachment. Left image: infrared reflectance image from spectral domain OCT image; green line indicates the position of the B-scan; middle image: B-scan SD-OCT image obtained in the enhanced depth (EDI)-mode showing cystoid macular edema, SND and numerous hyperreflective retinal spots (HRS) indicated with yellow arrows. The HRS were evaluated in the inner and outer retina within central 3mm (red vertical lines on OCT image delimitate area within 3000  $\mu\text{m}$ ); Right image: Microperimetry map showing decreased retinal sensitivity and central and stable fixation.

**Figure. 2.** Right eye of a patient with cystoid diabetic macular edema. Left image: infrared reflectance image from spectral domain OCT image; green line indicates the position of the B-scan; middle image: B-scan SD-OCT image obtained in the EDI-mode showing cystoid macular edema, hyperreflective retinal spots (HRS) indicated with yellow arrows. The HRS were evaluated in the inner and outer retina within central 3mm (red vertical lines on OCT image delimitate area within 3000  $\mu\text{m}$ ); Right image: Microperimetry map showing decreased retinal sensitivity and central and stable fixation.



**Table 1. Morphologic parameters**

Variable	Subfoveal neuroretinal detachment		P-value*
	No	Yes	
<b>Macula thickness</b>			
CMT (μm)	499.5±116.7	576.0±174.4	<b>0.0320</b>
CRT (μm)	499.5±116.7	460.6±145.6	0.2315
<b>Temporal RT</b>			
Inner 500 μm	256.9±77.9	286.0±139.3	0.2616
Outer 500 μm	181.8±69.9	207.5±66.3	0.1486
Total 500 μm	508.3±107.8	566.4±161.0	0.0759
Inner 1500 μm	229.2±51.5	260.5±75.6	<b>0.0442</b>
Outer 1500 μm	143.9±72.5	172.4±64.3	0.1168
Total 1500 μm	430.3±117.5	500.9±130.7	<b>0.0264</b>
<b>Nasal RT</b>			
Inner 500 μm	243.4±81.3	271.1±83.5	0.1913
Outer 500 μm	159.5±71.8	159.3±53.3	0.9925
Total 500 μm	480.8±113.9	530.3±139.0	0.1176
Inner 1500 μm	233.6±46.9	253.8±77.5	0.1751
Outer 1500 μm	101.3±41.5	130.2±61.8	<b>0.0228</b>
Total 1500 μm	411.7±84.5	446.8±70.3	0.0926
<b>Choroidal thickness</b>			
Fovea	206.5±57.4	238.4±52.2	<b>0.0285</b>
Temporal 500 μm	205.3±58.6	230.9±52.7	0.1102
Temporal 1500 μm	198.0±60.6	230.8±60.2	0.0841
Nasal 500 μm	200.9±60.3	224.5±48.4	<b>0.0003</b>
Nasal 1500 μm	170.9±48.7	222.0±60.3	<b>0.0378</b>
Total	196.3±48.9	229.3±48.0	<b>0.0098</b>
<b>HRS</b>	79.7±22.8	100.6±12.2	<b>&lt;0.0001</b>

\*) t-test for independent samples.

Legend: CMT- central macular thickness; CRT- central retinal thickness excluding subfoveal neuroretinal detachment; RT- retinal thickness; inner- inner retinal thickness from the inner limiting membrane to the outer plexiform layer; outer- outer retinal thickness from the outer nuclear layer to the retinal pigment epithelium; HRS- hyper-reflective retinal spots; Total- mean value from all measured points.



**Table 2. Functional parameters**

<i>Variable</i>	<i>Subfoveal neuroretinal detachment</i>		<i>P-value</i>
	<i>No</i>	<i>Yes</i>	
BCVA (ETDRS letters, Mean $\pm$ SD)	59.0 $\pm$ 13.8	55.8 $\pm$ 12.4	0.3434 <sup>a</sup>
Retinal sensitivity 4°, (dB, Mean $\pm$ SD)	10.0 $\pm$ 4.4	4.5 $\pm$ 4.4	<b>0.0024<sup>a</sup></b>
Retinal sensitivity 12°, (dB, Mean $\pm$ SD)	12.8 $\pm$ 3.9	8.7 $\pm$ 5.0	<b>0.0152<sup>a</sup></b>
Site of fixation, number of patients			0.1902 <sup>b</sup>
Central	48 (96%)	18 (81.8%)	
Relatively Eccentric	2 (4%)	4 (18.2%)	
Fixation stability, number of patients			<b>0.0035<sup>b</sup></b>
Unstable	4 (8%)	0 (0%)	
Relatively Unstable	4 (8%)	13 (59.1%)	
Stable	42 (84%)	9 (40.9%)	

a) t-student test for independent samples; b) Fisher's exact test.

Legend: BCVA- Best Corrected Visual Acuity; dB- decibels; SD- standard deviation;

**Table 3. Spearman correlation coefficients among choroidal thickness, retinal sensitivity 12°, and hyper-reflective retinal spots in patients with and without subfoveal neuroretinal detachment.**

		RS 12°	Total number of HRS
<i>Patients without SND</i>	Choroidal thickness	<b>0.455<sup>a</sup></b> (0.022)	<b>-0.262<sup>b</sup></b> (0.066)
	RS 12°		<b>-0.415<sup>c</sup></b> (0.039)
<i>Patients with SND</i>	Choroidal thickness	<b>-0.365</b> (0.300)	-0.097 (0.667)
	RS 12°		0.198 (0.583)

Coefficients clinically significant ( $\rho > 0.20$ ) are reported in bold character. *P*-value of the statistical test in brackets.

<sup>a</sup> Effect of SND on the relationship between Choroidal thickness and Retinal sensitivity (RS):  $P=0.003$ ; <sup>b</sup> Effect of SND on the relationship between Total number of HRS and Choroidal thickness:  $P=0.443$ ; <sup>c</sup> Effect of SND on the relationship between Total number of HRS and Retinal sensitivity (RS):  $P=0.003$

Legend: SND- subfoveal neuroretinal detachment; RS 12°- retinal sensitivity within 12 central degrees; HRS- hyper-reflective retinal spots

**Tab. 4 - Correlation between subfoveal neuroretinal detachment thickness and morphological and functional parameters**

Total CT	CMT	CRT	BCVA	RS 4°	RS 12°
-0.144	0.186	0.035	-0.341	<b>-0.394<sup>a</sup></b>	<b>-0.497<sup>b</sup></b>

<sup>a</sup>  $P=0.070$  borderline; <sup>b</sup>  $P=0.019$

**Spearman correlation coefficient**

Legend: Total CT- mean choroidal thickness (mean value from all measured points); CMT- central macular thickness; CRT- central retinal thickness excluding subfoveal neuroretinal detachment; BCVA- best corrected visual acuity; RS 4° retinal sensitivity within central 4 degrees; RS 12° retinal sensitivity within central 12 degrees;

